Environ. Sci. Technol. **2000**, *34,* 211−217

Particle Detection Efficiencies of Aerosol Time of Flight Mass Spectrometers under Ambient Sampling Conditions

JONATHAN O. ALLEN,[†] DAVID P. FERGENSON,[‡] ERIC E. GARD,[‡,§] LARA S. HUGHES,[†] BRADLEY D. MORRICAL,[‡] MICHAEL J. KLEEMAN,[†,⊥] DEBORAH S. GROSS,[‡,∥] MARKUS E. GÄLLI,[‡,⊗] KIMBERLY A. PRATHER,[‡] AND GLEN R. CASS*,[†]

Environmental Engineering Science Department, California Institute of Technology, Pasadena, California 91125, and Department of Chemistry, University of California, Riverside, Riverside, California 92521

Aerosol time-of-flight mass spectrometers (ATOFMS) measure the size and chemical composition of single aerosol particles. To date, these instruments have provided qualitative descriptions of aerosols, in part because the fraction of particles actually present in the atmosphere that is detected by these instruments has not been known. In this work, the particle detection efficiencies of three ATOFMS instruments are determined under ambient sampling conditions from the results of colocated sampling with more conventional reference samplers at three locations in southern California. ATOFMS particle detection efficiencies display a power law dependence on particle aerodynamic diameter (D_a) over a calibration range of $0.32 < D_a < 1.8$ microns. Detection efficiencies are determined by comparison of ATOFMS data with inertial impactor data and are compared to detection efficiencies determined independently by the use of laser optical particle counters. Detection efficiencies are highest for the largest particles and decline by approximately 2 orders of magnitude for the smallest particles, depending on the ATOFMS design. Calibration functions are developed here and applied to scale ATOFMS data to yield continuous aerosol mass concentrations as a function of particle size over an extended period of time.

Introduction

One long-standing goal of atmospheric aerosol science has been to determine the extent to which airborne particles of the same size differ in chemical composition. Recently developed aerosol time-of-flight mass spectrometer (ATOFMS) instruments now are capable of determining the size and chemical composition of single particles (*1, 2*). To date, field sampling data from these instruments have been used qualitatively to study both the sources and transformations of atmospheric particles (*3*−*6*). The need exists to devise calibration techniques to *quantitatively* reconstruct continuous time series of the actual size distribution and chemical composition of atmospheric aerosols from ATOFMS data. Toward this end, the absolute particle detection efficiencies of ATOFMS instruments under field sampling conditions are determined in the present paper.

Aerosol beams are generated in an ATOFMS instrument by supersonic expansion of the aerosol. Particles within this aerosol beam are sized according to their velocities as they pass timing lasers located downstream of the expansion nozzle. Knowing the velocity of a specific particle, a desorption/ionization laser is then fired to intercept the particle creating ions which are measured in a time-of-flight mass spectrometer. The transmission efficiency of particles through a supersonic expansion, defined as the fraction of the particles that is focused into the particle beam downstream of the expansion nozzle, has been measured (*7*−*10*) and modeled (*10*). These authors observed a maximum transmission efficiency for particle sizes for which the nozzle had been designed and a sharp decrease in transmission efficiency for larger and smaller particles. These studies have been useful in the design of ATOFMS instruments and explain why particle counting efficiency varies as a function of particle size. But nozzle transmission efficiency is only one of several factors that contribute to the probability that a particular atmospheric particle will be detected; other factors include the probability that the particle will be detected by the timing lasers that measure its velocity (hence size) and the probability that the particle will be successfully hit by the desorption/ionization laser.

Here we report on the detection efficiency of ATOFMS instruments for atmospheric aerosols as determined by comparison of ATOFMS data with data from more conventional reference samplers. These data are from an atmospheric aerosol field sampling experiment conducted at three sites in southern California (*11, 12*). At each site, colocated sampling was performed over a 2-week period using an ATOFMS instrument, filter-based samplers, cascade impactors, and an optical particle counter. Aerosol mass and number concentrations determined from the ATOFMS-detected particles are compared to ambient aerosol mass and number concentrations measured using cascade impactors and optical particle counters. From these comparisons, the particle detection efficiencies of the ATOFMS instruments as a function of particle size are determined by nonlinear regression. Continuous atmospheric aerosol mass concentrations as a function of particle size are then reconstructed by applying these detection efficiency factors to the ATOFMS data.

Experimental Method

Ambient aerosols were sampled with ATOFMS and reference sampling instruments at three sites in southern California between September 21 and October 2, 1996. This study was designed to observe particle transport and transformation at the single particle level as air parcels were advected from over the Pacific Ocean and across southern California in the presence of urban emission sources (*11, 12*). The sampling sites were located near the coast at Long Beach, CA; 22 km

* Corresponding author phone: (626)395-6888; fax: (626)395-2940; e-mail: glen@eql.caltech.edu.
[†] California Institute of Technology.
[‡] University of California, Riverside.
[§] Present address: Lawrence Livermore National Laboratory, 7000 East Avenue Mail Stop L-232, Livermore, CA 94550.
[⊥] Present address: Civil & Environmental Engineering, University of California, Davis, CA 95616.
[∥] Present address: Department of Chemistry, Carleton College, 1 North College Street, Northfield, MN 55057.
[⊗] Present address: TSI, Inc., P.O. Box 64394, St. Paul, MN 55164.

10.1021/es9904179 CCC: $19.00
Published on Web 12/01/1999

TABLE 1. Colocated Sampling Events

date	time (PDT)	location	ATOFMS
23 Sep 96	0700−1100	Long Beach	transportable
23 Sep 96	1500−1900	Riverside	laboratory
24 Sep 96	0700−1100	Long Beach	transportable
24 Sep 96	1500−1900	Riverside	laboratory
25 Sep 96	1500−1900	Riverside	laboratory
26 Sep 96	1500−1900	Riverside	laboratory
01 Oct 96	0700−1100	Long Beach	transportable
01 Oct 96	1100−1500	Fullerton	transportable
02 Oct 96	0700−1100	Long Beach	transportable
02 Oct 96	1100−1500	Fullerton	transportable

inland from Long Beach at Fullerton, CA; and 50 km inland from Fullerton at Riverside, CA. At Long Beach and Fullerton, the ATOFMS and electronic aerosol instruments sampled for two 48-h periods. The ATOFMS instruments at these sites were transportable units described by Gard et al. (*13*). At Riverside the ATOFMS and electronic aerosol instruments were operated continuously for the first week of the 2-week period. The ATOFMS instrument at this site was the laboratory unit described by Noble and Prather (*14*). Filter samplers and impactors were operated on selected days at each site over 4-h intensive sampling periods: 0700−1100 h PDT at Long Beach, 1100−1500 at Fullerton, and 1500−1900 at Riverside. Data from 10 intensive sampling events are analyzed in this work (see Table 1).

The operation of the ATOFMS instruments is described elsewhere (*13*−*15*); the ATOFMS particle detection method is summarized here. Sampled aerosol is introduced into the laboratory instrument at atmospheric pressure and a flow rate of 20 $cm^3 s^{-1}$ (*14*, *15*). The aerosol flow is directed through an expansion nozzle and three skimmers. During the expansion, particles are accelerated to a velocity characteristic of their aerodynamic size, with the smallest particles traveling at the highest speeds. After the last skimmer, velocities (hence aerodynamic size) of individual particles are measured in the sizing chamber by detecting scattered light from two timing lasers positioned a known distance apart.

The rarefied aerosol is subsequently directed into the desorption/ionization chamber of the ATOFMS instrument. The arrival time of a specific particle is predicted based on the velocity measured in the sizing chamber, and a desorption/ionization laser is fired to intercept the moving particle. Ionized fragments from the particle are directed to a time-of-flight mass spectrometer. The particle size and, if present, mass spectrum are then recorded on a personal computer. Particles which are detected by both timing lasers are said to have been "sized"; those which are also desorbed and ionized by the third laser to produce mass spectra are said to have been "hit".

The design of the transportable instruments is slightly different from that of the laboratory instrument (*13*). Relevant to this work, the transportable units have one expansion nozzle and two skimmers. Differences in the flow of the expanding aerosol result in different particle terminal velocities and transmission efficiencies for the laboratory and transportable ATOFMS instruments.

Incorrectly-sized particles are occasionally recorded by the ATOFMS instruments. This is sometimes due to coincident particles in the sizing chamber. In this case one particle scatters light from the first timing laser, and another particle scatters light from the second timing laser before the original particle arrives at the beam of the second laser. The measured velocity in this case is greater than the original particle's actual velocity. As a result, the desorption/ionization laser is fired too early, and a mass spectrum is not acquired for the particle. Thus, although many correctly sized particles are not hit, hit particles are very unlikely to have been incorrectly sized. The detection efficiency factors developed here use only data for hit particles.

The relationship between aerodynamic particle size and particle velocity in the sizing chamber was measured in the laboratory prior to the field experiment for each instrument. Monodisperse aerosols of 0.26−1.0 μm diameter polystyrene latex spheres were generated with a nebulizer. Monodisperse ammonium sulfate particles were generated with a vibrating orifice aerosol generator in the range 1.1−6.6 μm from a 50/50 volume methanol/water solution. These particles, with densities of 1.0 and 1.7 g/cm^3, exhibited the same dependence of velocity on aerodynamic diameter, D_a. For the laboratory ATOFMS, a calibration curve expressing the relationship between particle velocity and D_a was fitted to a third-order polynomial in inverse velocity (*14*). For the transportable ATOFMS instruments, the relationship between particle velocity and D_a was fitted to a power-law in velocity (*13*). The fitted functions are nearly identical for both transportable instruments; this is expected since these instruments have identical designs.

After a particle has been detected, the ATOFMS instrument processes and saves the particle data. During this time the ATOFMS instrument electronic system is busy and cannot detect new particles. The busy time has been measured to be 130 ms for particles which were sized but not hit and 634 ms for hit particles. The saving time for hit particles was also observed to increase linearly with the number of particles previously saved to the storage disk. Subsequent to the sampling experiment, the time spent processing and saving data was calculated for each hour of the field experiment. This busy time was then deducted from the apparent ATOFMS sampling time for each hour.

The reference method samplers at each site included filter samplers, inertial impactors, optical particle counters (at Long Beach and Riverside), and electrical aerosol analyzers. The operation of these samplers and the sample analyses are summarized here; detailed descriptions are presented elsewhere (*11*). Fine particles were collected on Teflon filters downstream of AHIL-design cyclone separators (*16*) which removed coarse particles (D_a > 2.2 μm). Two 10-stage microorifice impactors (MOI) (MSP Corporation, Minneapolis, MN, Model 110) (*17*) were operated at each site. Teflon-coated AHIL-design cyclone separators were operated upstream of the impactor inlets to remove coarse particles (D_a > 1.8 μm). Particles were collected on aluminum impaction substrates in one of the MOIs and on Teflon impaction substrates in the other. In order to avoid sample contamination, no coatings were applied to the impaction substrates. The fine particles in the Los Angeles atmosphere are generally sticky enough to avoid particle bounce problems within the impactor. Coarse particles, which may be more likely to bounce off their intended impaction stage, were removed to prevent the contamination of the fine particle samples. The impaction substrates and filters were weighed before and after sampling on a mechanical microgram balance (Mettler Model M-55-A) in a temperature and humidity-controlled in room (21.0 ± 0.5 °C, 37 ± 3% RH) to determine the distribution of aerosol mass as a function of particle size.

Laser optical particle counters (Particle Measuring Systems, Model ASASP-X) were operated continuously at the Long Beach and Riverside sites. Every 5 s these units recorded the number of particles in 31 size bins spanning the particle diameter range 0.11−2.55 μm.

Results and Discussion

The objective of this work is to determine the particle detection efficiencies of the ATOFMS instruments by comparison with reference sampler data. Mass measurement of cascade impactor samples is the most direct method to

determine the aerosol mass distribution as a function of particle size. Impactor mass data are particularly useful for the calibration of ATOFMS counting efficiencies because both the impactors and ATOFMS instruments segregate particles based on their aerodynamic diameters and operate over an overlapping aerodynamic size range, 0.32−1.8 μm. The aerosol mass concentration measured for a sample collected on stage i of a cascade impactor is designated m_i. This is deemed to be the reference measurement of the aerosol mass between the upper and lower cut-off diameters of the impactor stage.

Laser optical particle counters (OPCs) measure the aerosol number concentration and particle sizes from scattered light intensities. The relationship between light scattering intensity and the physical size of particles has been shown to depend on particle chemical composition (*18*, *19*). The ambient aerosol calibration of Hering et al. (*18*, *20*) was used to calculate particle sizes based on light scattering intensity. Particle mass distributions then were computed assuming spherical particles with a density of 1.3 g cm^{-3}.

Over the period of the study, the three ATOFMS instruments sized and collected mass spectra on 3.13 × 10^5 atmospheric particles. Velocity and sampling time data were recorded for each of these particles. Particle aerodynamic diameters, D_a, were determined from the laboratory calibration curves that relate particle velocity to D_a as discussed above. From these data, the apparent aerosol number concentration in a particle size bin j, n_j^*, was calculated as the sum of particles hit by an ATOFMS in the size range $D_{a,j} < D_a < D_{a,j+1}$ divided by the volume of air sampled. For comparison with impactor data, the size range of particles included in each ATOFMS size bin j were conveniently chosen so that an integral number of narrower ATOFMS bins fit within each impactor bin i.

If particles are assumed to be spherical and of uniform density, the apparent aerosol mass concentration in a narrow ATOFMS particle size bin j, m_j^*, is

$$m_j^* = n_j^* \frac{\pi}{6} \rho_p \overline{D_{p,j}}^3 \tag{1}$$

where ρ_p is the particle density and $\overline{D_{p,j}}$ is the logarithmic mean particle diameter in size bin j. The density of particles detected by the ATOFMS instruments and OPCs is assumed to be 1.3 g cm^{-3}, a value between the densities of inorganic substances such as ammonium sulfate and the densities of organic liquids and water which have specific gravities close to unity. Here we subdivide each impactor bin i into 10 ATOFMS size bins j. The ratio of the upper to lower particle size limit for each of these bins is approximately 1.06, which is sufficiently small so that $\overline{D_{p,j}}$ is an accurate representation of particle size over the entire size bin.

Equation 1 is more conveniently expressed in terms of the average aerodynamic diameter $\overline{D_{a,j}}$. The relation between D_p and D_a is (*21*)

$$D_p = D_a \left(\frac{\rho_1 C_c(D_a)}{\rho_p C_c(D_p)} \right)^{1/2} \tag{2}$$

where ρ_1 is unit density (1 g cm^{-3}) and C_c is the slip correction factor as a function of particle diameter for flow in the transition regime. After substitution eq 1 becomes

$$m_j^* = n_j^* \frac{\pi}{6 \rho_p^{1/2}} \left(\frac{\rho_1 C_c(D_a)}{C_c(D_p)} \right)^{3/2} \overline{D_{a,j}}^3 \tag{3}$$

Apparent aerosol mass concentrations then may be compared with data from the reference method samplers.

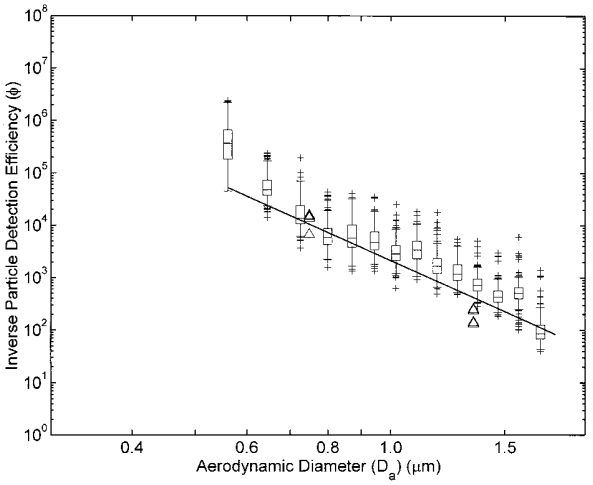

FIGURE 1. Inverse particle detection efficiency (ϕ) versus aerodynamic diameter (D_a) for the transportable ATOFMS instrument sampling ambient aerosols at Long Beach based on comparisons with impactor (△) and OPC (box and whisker) measurements. The solid line represents the best power law fit to the impactor data according to eqs 6 and 7. Note that the △ symbols are plotted at the logarithmic mean D_a value within each impactor bin but apply across the entire width of the impactor bin (see text).

One measure of the particle detection efficiency of an ATOFMS instrument is the ratio of aerosol mass as measured with an impactor to that estimated from ATOFMS data, ϕ_{MOI}, calculated as

$$\phi_{MOI} = \frac{m_i}{\sum_j C_i m_j^*} \tag{4}$$

Note that ϕ is the inverse of the particle mass detection efficiency. A similar measure of particle detection efficiency relative to OPC data is

$$\phi_{OPC} = \frac{m_k}{m_k^*} \tag{5}$$

where m_k is the aerosol mass concentration in OPC bin k and m_k^* is the apparent aerosol mass concentration measured by an ATOFMS in the same particle size bin k. Since the particle size bins for the OPC and ATOFMS data are narrow and identical, eq 5 is equivalent to the ratio of the aerosol number concentrations measured by the OPC and ATOFMS. Values of ϕ_{MOI} from the intensive sampling periods are plotted in Figures 1 and 2. Note that ϕ_{MOI} is plotted in these figures with triangular symbols located in the logarithmic center of each impactor bin, although the value of ϕ_{MOI} is in fact distributed over the entire width of the respective impactor bin. Values of ϕ_{OPC} were calculated for each hour of the study; these data are shown as box and whisker plots over narrow size ranges in these figures. Each box shows the second and third quartile range with a line at the median value. Whiskers extend from the quartile boundaries to two times the distance from the quartile boundary to the median. Crosses mark data points which lie outside the whiskers.

For the transportable instrument at Long Beach, values of ϕ determined by independent comparison with impactor and OPC data are identical within experimental error (see Figure 1); ϕ values lie in the range 10^2−10^6 for particles with 0.56 < D_a < 1.8 μm. Values of ϕ show a strong dependence on D_a; as particle size is reduced, a smaller fraction of the

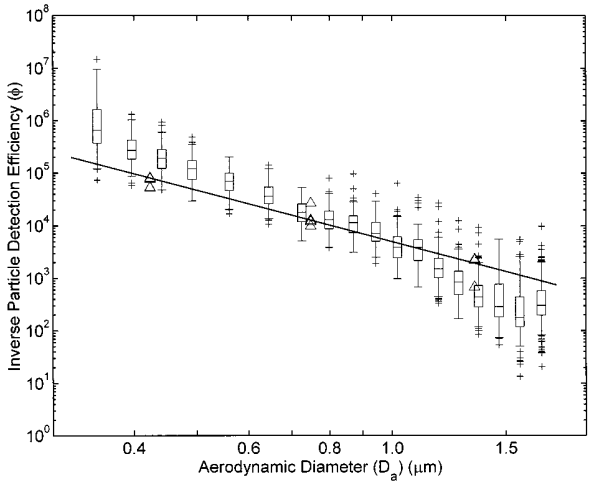

FIGURE 2. Inverse particle detection efficiency (ϕ) versus aerodynamic diameter (D_a) for the laboratory ATOFMS instrument sampling ambient aerosols at Riverside based on comparisons with impactor (△) and OPC (box and whisker) measurements. The solid line represents the best power law fit to the impactor data according to eqs 6 and 7. Note that the △ symbols are plotted at the logarithmic mean D_a value within each impactor bin but apply across the entire width of the impactor bin (see text).

particles actually present in the atmosphere are detected. The dependence of log ϕ on log D_a is approximately linear for both the impactor and OPC data. Data for the transportable ATOFMS operated at Fullerton (not shown) are similar to those shown in Figure 1. This is expected since the unit at Fullerton had the same design as the one at Long Beach.

For the laboratory ATOFMS, median ϕ values lie in the range 10^2-10^6 for particles with $0.32 < D_a < 1.8$ μm (see Figure 2). Values of ϕ_{MOI} lie within the range of experimentally determined values of ϕ_{OPC}, although the value of ϕ_{MOI} appears to be greater than ϕ_{OPC} for large particles and less than ϕ_{OPC} for small particles. A likely explanation for this is that the aerosol at Riverside is much more heterogeneous in origin than the marine aerosol at Long Beach. At Riverside large particles, e.g. soil dust, are expected to have densities greater than the assumed density ($\rho = 1.3$ g cm^{-3}) used to convert the ATOFMS particle counts into mass concentration values, and small particles, e.g. organic particles, are expected to have densities smaller than the assumed density ($\rho = 1.3$ g cm^{-3}). As at Long Beach, the dependence of log ϕ on log D_a is approximately linear over this particle size range.

It should be noted that the sampling biases shown in Figures 1 and 2 are advantageous for the accurate determination of aerosol concentration and chemical composition with the ATOFMS instruments. This is because the ATOFMS instruments detect approximately 2 particles per s and hit approximately 10% of these particles. For a typical urban aerosol, the number concentration of accumulation mode particles ($0.32 < D_a < 1.8$ μm) is approximately 10^3 cm^{-3}. In addition, number distributions for accumulation mode aerosols show an approximately exponential increase in the number of particles as the particle size decreases. Thus, approximately 2×10^4 accumulation mode particles are introduced into the ATOFMS each second, and the vast majority of these particles have sizes toward the lower limit of the particle size range, i.e., $D_a \approx 0.3$ μm. Because only a small fraction of the sampled aerosol particles can be sized and hit by the ATOFMS, if sampling were not strongly biased against smaller particles, then only these more numerous smaller particles would be detected. Thus, sampling should be biased so that some particles of all sizes are detected with reasonable frequency. For a representative determination of aerosol mass concentration, it is convenient for the likelihood of sampling a particle to be proportional to the particle mass, i.e. approximately proportional to D_a^3, or $\phi \propto D_a^{-3}$.

We hypothesize that the ATOFMS particle counts can be reliably scaled by ϕ to yield atmospheric aerosol concentrations and that the scaling functions are dependent only on D_a. These hypotheses can be expressed as a testable model by rearrangement of eq 4 to

$$m_i = \sum_{j \subset i} \phi(D_{a,j}) m_j^* + \epsilon_i \qquad (6)$$

where $\phi(D_{a,j})$ is the scaling function and ϵ_i is the residual aerosol mass concentration. Plots of ϕ versus D_a suggest that ϕ follows a power law relationship in D_a (see Figures 1 and 2)

$$\phi = \alpha D_a^{\beta} \qquad (7)$$

The observed power law dependence of particle detection efficiency on particle size is similar to that observed for particle transmission through supersonic expansion nozzles like those used in the ATOFMS instruments (*7*).

Parameters α and β in eq 7 were determined by nonlinear regression of impactor mass concentration data on ATOFMS particle data with the ATOFMS particle data segregated into 10 narrow size intervals within each impactor size bin. Data from each ATOFMS were analyzed separately. Nonlinear regression analyses were conducted using the Matlab statistics package (The MathWorks, Natick, MA) (*22*). Fitted values of α and β are given in Table 2. The fitted scaling functions are shown as lines in Figures 1 and 2. Recall that the values of ϕ_{MOI} are average values plotted in these figures with triangular symbols located at the logarithmic center of the impactor bins, but, in fact, values of m_j^* are distributed over the entire width of their respective impactor bins. Since the actual values of $\alpha D_{a,j}^{\beta} m_j^*$, which are defined for 10 small size intervals per impactor bin, were used in the regression analyses rather than the single average value represented by the triangular symbols in Figures 1 and 2, the curves fit to eqs 6 and 7 do not necessarily pass through the triangle symbols in these figures.

Although the density and morphology of particles are expected to affect the efficiency with which individual particles are detected, it is unknown whether chemical composition significantly affects particle detection efficiencies averaged over the entire aerosol. We have assumed that the scaling functions, ϕ, are not affected by chemical composition, and this assumption can be tested by examining the correlation of the residuals from eq 6 with the measured chemical properties of the aerosol. Extensive aerosol composition data are available from chemical analyses of the impactor samples collected during the intensive sampling periods (*11*, *12*). Correlation coefficients of the residuals from eq 6 with the aerosol concentrations of individual chemical species were calculated for all of the chemical species which were measured at concentrations significantly above their detection limits in all of the impactor samples. The correlation coefficient squared (r^2) is the fraction of the variance of the residuals in eq 6 that is explained by a linear relationship with the concentration of a particular aerosol chemical species. The largest r^2 value for the data collected at Long Beach was 0.41 for Co (see Table 3). This apparent correlation is largely due to a single data point and is not strong evidence that the particle detection efficiency depends on Co concentration. Plots of residuals versus elemental carbon, organic carbon, NO_3^-, Na, and Sb for this site are similar to the results for Co. For all other aerosol species at Long Beach, $r^2 < 0.10$. For the Riverside site, all of the r^2 values were less than 0.10. These results indicate that the particle detection efficiencies

TABLE 2. Parameter Values Fit to the Scaling Function $\phi = \alpha D_a^{\beta}$

ATOFMS design	site	α[a]	β[a]	applicable range of D_a (μm)
transportable	Long Beach	2133 ± 501	-5.527 ± 0.861	0.56−1.8
transportable	Fullerton	2896 ± 1247	-5.500 ± 1.157	0.56−1.8
laboratory	Riverside	4999 ± 998	-3.236 ± 0.520	0.32−1.8

[a] Most likely parameter values and 95% confidence intervals.

TABLE 3. Correlation Coefficients Squared (r^2) for Residual Aerosol Mass Concentrations and Aerosol Concentrations of Individual Analytes

	r^2	
analyte	Long Beach	Riverside
mass	0.08	0.03
elemental carbon	0.21	0.005
organic carbon	0.38	0.04
NH_4^+	0.08	0.02
NO_3^-	0.36	0.01
SO_4^{2-}	0.04	0.09
Na	0.14	0.00
Al	0.06	0.001
Cl		0.03
V		0.03
Co	0.41	0.001
Zn	0.008	0.002
Sb	0.14	0.03
Au	0.05	0.07

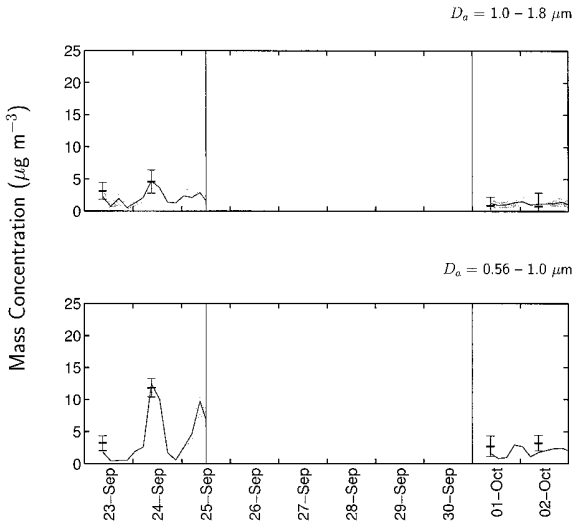

FIGURE 3. Continuous fine aerosol mass concentration as determined from the scaled ATOFMS data aggregated over impactor size bins and compared to impactor data at Long Beach. Scaled ATOFMS data are shown as a solid line with shading to indicate the 95% confidence intervals; impactor data are shown as heavy horizontal bars of 4-h duration with error bars indicating 2 SD.

did not depend on aerosol composition. Residual aerosol mass concentrations not explained by the model may be due to experimental errors in the aerosol mass concentrations measured by gravimetric analysis of impactor substrates or due to minor variations in instrument operation during the experiment.

One application of the scaling functions developed from data for the intensive sampling periods is to recreate the time series of aerosol concentrations from the ATOFMS data over the entire study period. The scaling functions can be used to estimate the continuous aerosol mass concentration

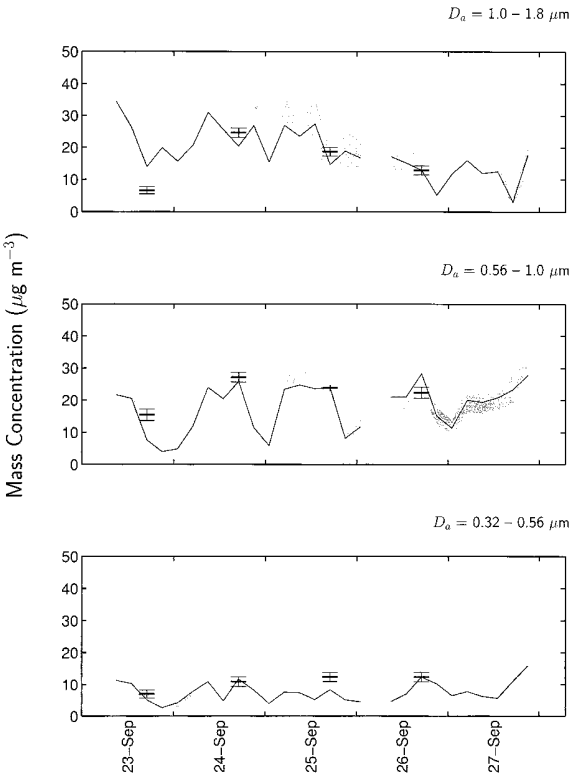

FIGURE 4. Continuous fine aerosol mass concentration as determined from the scaled ATOFMS data aggregated over impactor size bins and compared to impactor data at Riverside. Scaled ATOFMS data are shown as a solid line with shading to indicate the 95% confidence intervals; impactor data are shown as heavy horizontal bars of 4-h duration with error bars indicating 2 SD.

from the ATOFMS data as a function of particle size as follows

$$\hat{m}_i = \sum_{j \subset i} \phi m_j^* \tag{8}$$

where $\hat{m}_i$ is the estimate of the aerosol mass concentration in size range i for a particular time period. Confidence intervals can be placed on these estimates if they are made for the same particle size ranges and averaging times as the impactor data, i.e., MOI particle size bins with 4 h averaging times (*22*).

In Figures 3 and 4 the time series of fine aerosol mass concentrations are estimated from ATOFMS data over the same size ranges as employed by the impactors for the entire study period. Data from the Fullerton site are not shown since ATOFMS data are only available for approximately 48 h at that site. Also shown are the aerosol mass concentration data from the periodic impactor measurements. A comparison of the scaled ATOFMS and impactor data show that the error bounds on the measurements and estimates overlap during most of the intensive sampling periods. The general agreement between the scaled ATOFMS and impactor data indicate that the chosen scaling functions accurately translate

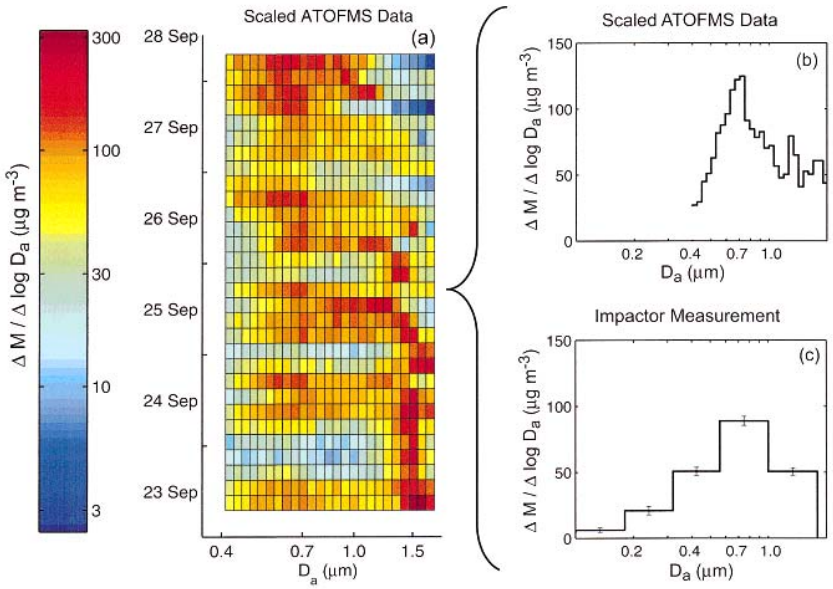

FIGURE 5. Aerosol mass distributions at Riverside: (a) time series based on scaled ATOFMS data for 4-h periods from September 23 though 28, 1996 with divisions at 0300, 0700, 1100, 1500, 1900, and 2300 h PDT, (b) scaled ATOFMS data for 1500−1900 h PDT on September 25, 1996, and (c) impactor measurements at the same time and place.

ATOFMS particle data into a time series of mass concentration data during the intensive sampling events.

Scaled ATOFMS data are available with temporal and particle size resolutions finer than those of the conventional samplers. Figure 5a shows the scaled ATOFMS data from Riverside binned into 4-h periods and 25 particle size intervals over the range $D_a = 0.42-1.8\,\mu$m. For comparison, that color coded graph of scaled ATOFMS data is translated in Figure 5b into a conventional plot of aerosol mass as a function of particle size for the intensive sampling event that occurred on the afternoon of September 25, 1996. Impactor measurement results for this sampling event are also shown for purposes of comparison in Figure 5c. The continuous data of Figure 5a show that the experiment began with relatively high supermicron aerosol concentrations on September 23 and 24. Later in the experiment, submicron particle concentrations are highest, especially on September 27 and 28. The high resolution size distribution data of Figure 5b show that the scaled ATOFMS data capture many of the detailed characteristics of the Los Angeles area aerosol including the pronounced peak in the submicron aerosol at ca. 0.7 μm particle diameter. That peak can be produced by secondary aerosol accumulation onto the nonsea salt background particles advected into the study region (*23*).

In addition to particle sizes, the ATOFMS instruments record mass spectra which indicate the chemical composition of single particles. The reconstruction of continuous time-series aerosol mass concentration and size distribution data from ATOFMS instrument records is a prerequisite to the complete reconstruction of size-resolved ambient aerosol chemical composition. The scaling functions developed here can be applied to increase the concentration of individual particles in proportion to the extent to which they were initially undercounted by the ATOFMS instruments. The mass spectra of these particles thus corrected for undercounting can next be compared to the chemical composition of the aerosol collected by the cascade impactors. The sensitivity of the ATOFMS instruments for individual chemical species present in the mixed ambient aerosols can then be determined from a comparison of the corrected ATOFMS data to impactor-based chemical composition data. The resulting chemical sensitivity factors which, when used with the particle scaling functions developed here, will allow the continuous and quantitative reporting of both aerosol size and chemical composition data from the ATOFMS instruments.

Acknowledgments

Financial support for this research was provided by the California Air Resources Board under agreement 95-305 (University of California, Riverside) and by the U.S. Environmental Protection Agency under EPA Grant R824970-01-0 (California Institute of Technology).

Literature Cited

(1) Johnston, M. V.; Wexler, A. S. *Anal. Chem.* **1995**, *67*, 721A.
(2) Wood, S. H.; Prather, K. A. *Trends Anal. Chem.* **1998**, *17*, 346−356.
(3) Liu, D. Y.; Rutherford, D.; Kinsey, M.; Prather, K. A. *Anal. Chem.* **1997**, *69*, 1808−1814.
(4) Gard, E. E.; Kleeman, M. J.; Gross, D. S.; Hughes, L. S.; Allen, J. O.; Morrical, B. D.; Fergenson, D. P.; Dienes, T.; Gälli, M. E.; Johnson, R. J.; Cass, G. R.; Prather, K. A. *Science* **1998**, *279*, 1184−1187.
(5) Murphy, D. M.; Anderson, J. R.; Quinn, P. K.; McInnes, L. M.; Brechtel, F. J.; Kreidenweis, S. M.; Middlebrook, A. M.; Pósfai, M.; Thompson, D. S.; Buseck, P. R. *Nature* **1998**, *392*, 62−65.
(6) Murphy, D. M.; Thompson, D. S.; Mahoney, M. J. *Science* **1998**, *282*, 1664−1669.
(7) Dahneke, B. E.; Cheng, Y. S. *J. Aerosol Sci.* **1979**, *10*, 257−274.
(8) Cheng, Y. S.; Dahneke, B. E. *J. Aerosol Sci.* **1979**, *10*, 363−368.
(9) Estes, T. J.; Vilker, V. L.; Friedlander, S. K. *J. Colloid Interface Sci.* **1983**, *93*, 84−94.
(10) Kievit, O.; Weiss, M.; Verheijen, P. J. T.; Marijnissen, J. C. M.; Scarlett, B. *Chem. Eng. Comm.* **1996**, *151*, 79−100.
(11) Hughes, L. S.; Allen, J. O.; Kleeman, M. J.; Johnson, R. J.; Cass, G. R.; Gross, D. S.; Gard, E. E.; Gälli, M. E.; Morrical, B. D.; Fergenson, D. P.; Dienes, T.; Noble, C. A.; Liu, D.-Y.; Silva, P. J.; Prather, K. A. *Environ. Sci. Technol.* **1999**, *33*, 3506−3515.
(12) Hughes, L. S.; Liu, D.-Y.; Allen, J. O.; Fergenson, D. P.; Kleeman, M. J.; Morrical, B. D.; Prather, K. A.; Cass, G. R. **1999**, submitted for publication in *Environ. Sci. Technol.*
(13) Gard, E.; Mayer, J. E.; Morrical, B. D.; Dienes, T.; Fergenson, D. P.; Prather, K. A. *Anal. Chem.* **1997**, *69*, 4083−4091.
(14) Noble, C. A.; Prather, K. A. *Environ. Sci. Technol.* **1996**, *30*, 2667−2680.

(15) Salt, K.; Noble, C. A.; Prather, K. A. *Anal. Chem.* **1996**, *68*, 230−234.
(16) John, W.; Reischl, G. *JAPCA* **1980**, *30*, 872−876.
(17) Marple, V. A.; Rubow, K. L.; Behm, S. M. *Aerosol Sci. Technol.* **1991**, *14*, 434−446.
(18) Hering, S. V.; McMurry, P. H. *Atmos. Environ.* **1991**, *25A*, 463−468.
(19) Kim, Y. J. *Aerosol Sci. Technol.* **1995**, *22*, 33−42.
(20) Hering, S. V. Personal communication, Aerosol Dynamics, Inc.
(21) Seinfeld, J. H.; Pandis, S. N. *Atmospheric Chemistry and Physics: From Air Pollution to Global Change*; Wiley-Interscience: 1998.
(22) Bates, D. M.; Watts, D. G. *Nonlinear Regression and Its Applications*; John Wiley & Sons: 1988.
(23) Kleeman, M. J.; Cass, G. R. *Atmos. Environ.* **1998**, *32*, 2803−2816.

Received for review April 13, 1999. Revised manuscript received September 7, 1999. Accepted October 12, 1999.

ES9904179